Combination of the cuproptosis inducer disulfiram and anti-PD-L1 abolishes NSCLC resistance by ATP7B to regulate the HIF-1 signaling pathway

PENGFEI LI[1], QI SUN[1], SHUPING BAI[2], HAITAO WANG[2] and LING ZHAO[2]

[1]Department of Radiology, [2]The Second Department of Respiratory, Harbin Medical University Cancer Hospital, Harbin, Heilongjiang 150040, P.R. China

Received March 6, 2023; Accepted September 25, 2023

DOI: 10.3892/ijmm.2023.5343

Abstract. Disulfiram (DSF) is used to treat non-small cell lung cancer (NSCLC). DSF significantly increases expression of programmed death-ligand 1 (PD-L1), which may enhance immunosuppression and immune escape of tumors. Therefore, the present study aimed to investigate the role of combined treatment of DSF and anti-PD-L1 in NSCLC resistance. The viability and apoptosis of A549 cells were detected by the Cell Counting Kit-8 assay and flow cytometry, respectively. The expression levels of ATPase copper-transporting β (ATP7B) and PD-L1 in A549 cells were detected by reverse transcription-quantitative PCR and western blot analysis. The levels of reactive oxygen species (ROS), malondialdehyde (MDA) and superoxide dismutase (SOD) in A549 cells were detected by respective assay kits. The expression levels of cuproptosis-associated proteins ferredoxin-1 (FDX1), ATP7B, solute carrier family 31 member 1 (SLC31A1), succinate dehydrogenase B (SDHB), PD-L1 and hypoxia inducible factor (HIF)-1A were analyzed by western blotting in A549 cells. DSF inhibited the viability of A549 cells and promoted expression levels of ATP7B and PD-L1 at both mRNA and protein levels in A549 cells. The viability of cisplatin (DPP)-treated A549 cells was increased following DSF treatment. JQ-1 (a PD-L1 inhibitor) suppressed the viability of DPP-treated A549 cells pretreated with DSF. DSF increased expression levels of ATP7B and PD-L1. The combination treatment of DSF and JQ-1 in A549 cells increased levels of ROS and MDA, as well as expression levels of FDX1 and SLC31A1; however, combination treatment decreased levels of SOD, as well as expression levels of ATP7B, SDHB, PD-L1, and HIF-1A. PX478 (an HIF-1 inhibitor) acted with DSF to enhance the inhibitory effects on the viability and on the induction of apoptosis of A549 cells. PX478 upregulated the levels of ROS and MDA, while it downregulated levels of SOD in DSF-treated A549 cells. PX478 promoted expression levels of FDX1 and SLC31A1, while it suppressed expression levels of ATP7B, PD-L1, and HIF-1A in DSF-treated A549 cells. In conclusion, the combined treatment of A549 cells with anti-PD-L1 and DSF enhanced the effect of cuproptosis on the inhibition of NSCLC cell viability.

Introduction

Lung cancer is one of the most common malignant tumors with the highest incidence and mortality worldwide in 2020, of which non-small cell lung cancer (NSCLC) accounts for ~85% of all lung cancer cases (1,2). The main types of NSCLC are adenocarcinoma and squamous and large cell carcinoma (3). Improved diagnosis, the availability of novel effective chemotherapeutic agents, advanced surgical techniques and declining smoking rates are contributing factors to gradually improving outcomes for NSCLC (4). However, the 5-year survival rate of patients with NSCLC is ~26% due to chemotherapy resistance (5). Cisplatin (DDP)-based therapy is the most widely used regimen for advanced NSCLC (6). Therefore, the reversal of DDP resistance should be addressed to improve the treatment efficacy of NSCLC.

Disulfiram (DSF), a drug used for the treatment of alcohol dependence, inhibits activity of aldehyde dehydrogenase 1 (ALDH1) (7). DSF promotes tumor cell apoptosis and inhibits tumor growth, tumor cell invasion and metastasis (8,9). In a clinical trial, DSF was shown to prolong survival in patients with metastatic NSCLC when added to a combination regimen of DDP and vinorelbine (10). An additional study indicated that DSF reverses DDP resistance in NSCLC by inhibiting ALDH1 expression (11). In view of the antitumor effect of DSF in NSCLC, it is necessary to explore its antitumor molecular mechanism of action.

DSF combined with copper (DSF/Cu) exhibits an antitumor effect, which could inhibit proliferation of a variety of tumor cells including melanoma, colorectal and lung cancer, glioma and breast cancer (12-14). The antitumor effect of DSF

Correspondence to: Dr Ling Zhao, The Second Department of Respiratory, Harbin Medical University Cancer Hospital, 150 Baojian Road, Nangang, Harbin, Heilongjiang 150040, P.R. China
E-mail: 1464@hrbmu.edu.cn

Key words: disulfiram, anti- programmed death-ligand 1, non-small cell lung cancer resistance, ATPase copper-transporting β, hypoxia inducible factor-1 signaling pathway

requires the participation of Cu^{2+}; its metabolite, diethyldithiocarbamate (DTC), *in vivo* forms chelate complexes with Cu^{2+} (CuET). CuET promotes coagulation of nuclear protein localization protein 4 and binds p97 protein, which affects its function in tumor cells and leads to CuET degradation, resulting in excessive accumulation of a large amount of waste protein in the cell, leading to the death of tumor cells (15). Cuproptosis is caused by direct binding of copper to the fatty acylated components of the tricarboxylic acid cycle, resulting in aggregation of fatty acylated proteins, loss of iron and sulfur cluster proteins and changes in mitochondrial respiration levels, which eventually leads to proteotoxic stress and cell death (16). Solute carrier family 31 member 1 (SLC31A1) and ATPase copper-transporting β (ATP7B), the key proteins of the cell membrane that control copper metabolism and homeostasis, trigger changes in intracellular copper concentration and are key factors that lead to cuproptosis (16). Zhou *et al* (17) demonstrated that DSF significantly upregulates expression of programmed death-ligand 1 (PD-L1) in hepatocellular cancer cells, which may enhance immunosuppression and immune escape of tumors. According to GEO database (ncbinlm.nih.gov/geo/), DSF significantly increased the level of ATP7B in hepatocellular carcinoma, which inhibits cuproptosis to a certain extent. Mi *et al* (18) indicated that downregulation of ATP7B expression downregulates the hypoxia inducible factor (HIF)-1 pathway, which downregulates PD-L1 expression. PX478, an experimental HIF-1 inhibitor, causes significant tumor regression and delays tumor growth in mice (19,20). PX478 inhibits HIF-1α protein levels and transactivation in a number of cancer cell lines (21). Cui *et al* (22) reported that a combination of PX-478 and anti-PD-L1 exerts a tumor inhibition effect compared with single treatment in lung carcinoma. Also, in renal cancer, subtype of succinate dehydrogenase B (SDHB), a ferric sulfur subunit protein of mitochondrial complex II that serves a key role in cuproptosis, is expressed at low levels and PD-L1 exhibits nearly undetectable expression. Low expression of the SDHB is one of the primary characteristics of cuproptosis, indicating that there may be an association between cuproptosis and PD-L1 expression (23).

Therefore, the present study aimed to investigate whether DSF upregulates the expression of ATP7B to activate the HIF-1 signaling pathway, thereby inducing the upregulation of PD-L1 expression and enhancing the effect of immunosuppression and immune escape of NSCLC. The present study aimed to assess whether the combined treatment of DSF with anti-PD-L1 could enhance the anticancer role of cuproptosis induction caused by single treatment of DSF in inhibiting NSCLC resistance.

Materials and methods

Cell culture. The human NSCLC cell line A549 was obtained from American Type Culture Collection (cat. no. CRM-CCL-185). The cells were cultured in RPMI-1640 supplemented with 10% fetal bovine serum (both Thermo Fisher Scientific, Inc.) at 37˚C with 5% CO_2.

Cell treatment. A549 cells were treated with DSF (0.1, 0.2, 0.5, 1.0 and 2.0 μM) in the presence or absence 0.2 μM $CuCl_2$ at 37˚C for 24 h. One experiment involved treatment of A549 cells with 2 μg/ml DDP in the presence or absence of DSF treatment at 0.1 and 1.0 μM for 48 h at 37˚C. An additional experiment involved treatment of A549 cells with 2 μg/ml DDP in the presence or absence of 1 μM DSF and 5 μM JQ-1 (PD-L1 inhibitor) for 48 h at 37˚C. Moreover, A549 cells were treated in the presence or absence of 1 μM DSF (0.2 μM Cu^{2+}) and 5 μM JQ-1 for 48 h at 37˚C. Finally, A549 cells were treated in the presence or absence of 1 μM DSF (0.2 μM Cu^{2+}) and 10 μM PX478 (HIF-1A inhibitor) for 48 h at 37˚C.

Cell Counting Kit-8 (CCK-8) assay. A549 cells were seeded in 96-well plates ($2x10^3$ cells/well) and continuously cultured at 37˚C for 24 h. Subsequently, cells were incubated with CCK-8 solution (10 μl; Beyotime Institute of Biotechnology) for 2 h at 37˚C with 5% CO_2. The absorbance of each well was detected by a spectrophotometer at 450 nm.

Reverse transcription-quantitative (RT-q)PCR. Total RNA was isolated from A549 cells using TRIzol® (Thermo Fisher Scientific, Inc.) according to the manufacturer's specification. cDNA was synthesized from RNA using the TransScript All-in-One First-Strand cDNA Synthesis kit (TransGen Biotech Co. Ltd.) according to the manufacturer's instructions. The relative expression levels of each gene were detected by qPCR using SYBR® Premix EX Taq™ kit (Takara Bio, Inc.) in an ABI 9600 (Applied Biosystems; Thermo Fisher Scientific, Inc.) thermal cycler according to the manufacturer's instructions and quantified by $2^{-\Delta\Delta Cq}$ (24). The following were the thermocycling conditions: Initial denaturation at 95˚C for 3 min; followed by 40 cycles of denaturation at 95˚C for 30 sec, annealing at 60˚C for 30 sec and extension at 72˚C for 30 sec. The primer sequences were as follows: ATP7B forward, 5'-CCTCCTCTC CCGGGACTTTA-3' and reverse, 5'-TGGCAAGTCATGCCC AAGAT-3'; PD-L1 forward, 5'-TTTGCTGAACGCCCCAT ACA-3' and reverse, 5'-GGAATTGGTGGTGGTGGTCT' and GAPDH forward 5'-GGGAAACTGTGGCGTGAT-3' and reverse, 5'-GAGTGGGTGTCGCTGTTGA-3'. GAPDH was used as an internal control.

Western blot analysis. A549 cells were collected, lysed in RIPA buffer (Beyotime Institute of Biotechnology, Shanghai, China) and centrifuged at 12,000 x g at 4˚C for 10 min to obtain supernatant. The levels of the proteins in the supernatant were analyzed by bicinchoninic acid protein assay kit. The protein (30 μg/lane) were separated by 10% SDS-PAGE, transferred onto a polyvinylidene fluoride membrane and blocked with 5% skimmed milk in 0.1% TBS-Tween-20 for 1 h at room temperature. The membranes were incubated with the following primary antibodies: ATP7B (cat. no. ab124973; 1:1,000; Abcam), PD-L1 (cat. 0no. ab213524; 1:1,000; Abcam), ferredoxin-1 (FDX1; cat. no. 12592-1-AP; 1:1,000; Proteintech), SLC31A1 (cat. no. ab129067; 1:1,000; Abcam), SDHB (cat. no. ab175225; 1:50,000; Abcam), HIF-1A (cat. no. #36169; 1:1,000; Cell Signaling Technology) and GAPDH (cat. no. ab9485; 1:2,500; Abcam) overnight at 4˚C. Subsequently, the membranes were washed with TBST and incubated with horseradish peroxidase-conjugated secondary antibody (cat. no. ab6721; 1:2,000; Abcam) for 1 h at room temperature. The protein bands were visualized by an enhanced chemiluminescence kit (Thermo Fisher Scientific,

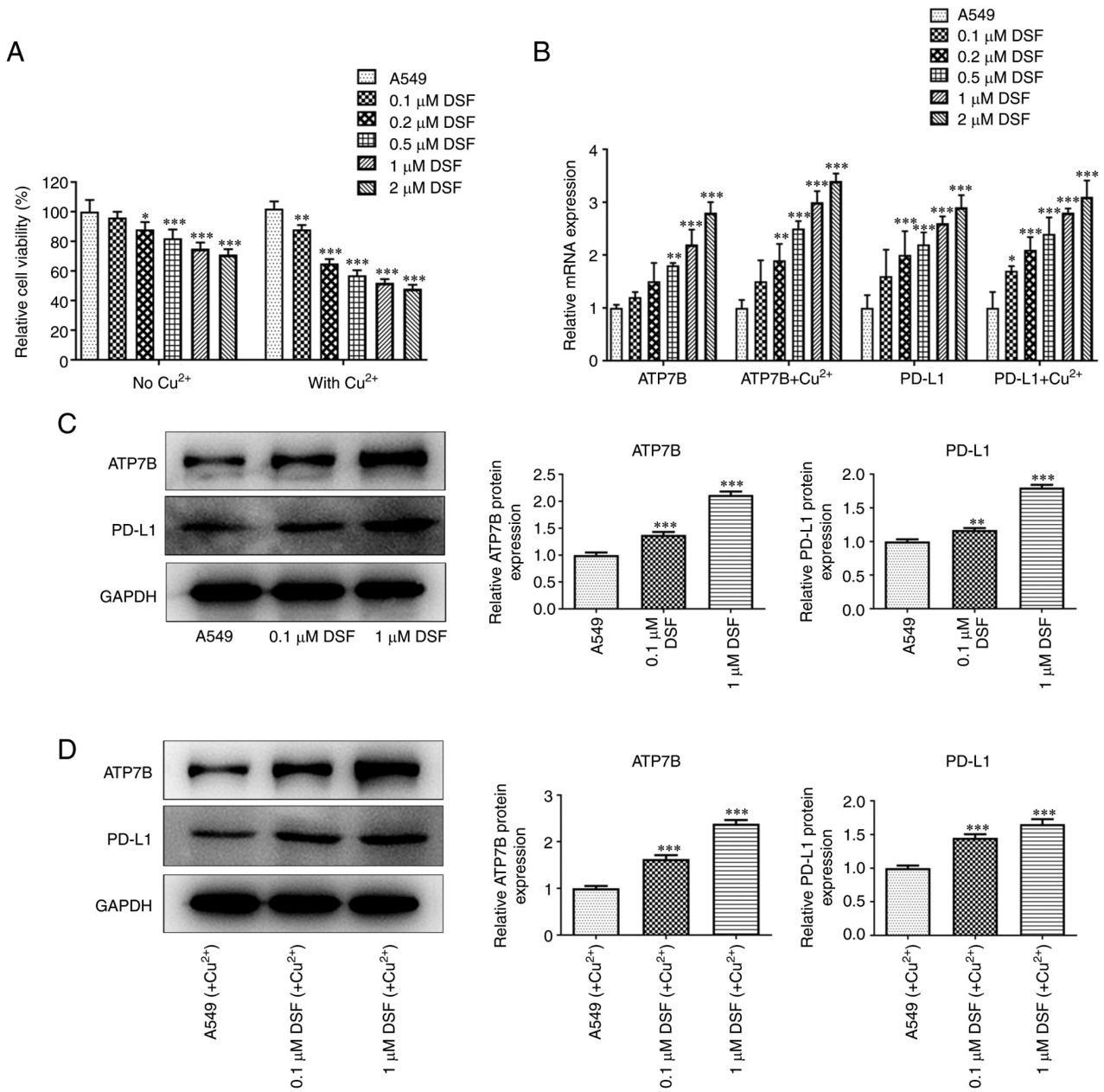

Figure 1. Effect of DSF on viability and expression of ATP7B and PD-L1 of A549 cells. (A) Viability of A549 cells treated with DSF and/or Cu^{2+} was detected by Cell Counting Kit-8 assay. (B) mRNA expression of ATP7B and PD-L1 in A549 cells treated with DSF and/or Cu^{2+} was detected by reverse transcription-quantitative PCR. (C) Expression of ATP7B and PD-L1 in A549 cells treated with DSF was detected by western blot. (D) The protein expression of ATP7B and PD-L1 in A549 cells treated with DSF and Cu^{2+} was detected by western blot. *P<0.05, **P<0.01 and ***P<0.001 vs. A549. DSF, disulfiram; ATP7B, ATPase copper-transporting β; PD-L1, programmed death-ligand 1.

Inc.) and quantified by Image J 1.8.0 software (National Institutes of Health).

Flow cytometry. The apoptosis of A549 cells was detected by flow cytometry using an Annexin V/propidium iodide (PI) kit (Guangzhou RiboBio Co., Ltd.). Briefly, A549 cells were collected and washed with ice-cold PBS twice. Subsequently, A549 cells were resuspended in 100 μl binding buffer ($2x10^5$ cells) and stained with 5 μl Annexin V and 5 μl PI at 4˚C for 15 min in the dark. Finally, a flow cytometer (FACSCalibur; BD Biosciences) and Flowjo vX.0.7 software (FlowJo LLC) were used to detect the apoptosis of A549 cells. The apoptotic rate was calculated using the formula: Apoptotic rate=Q2+Q3.

Detection of oxidative stress. A549 cells were lysed in cell lysis solution (Beyotime Institute of Biotechnology), then centrifuged at 10,000 x g at 4˚C for 10 min to obtain the cell supernatant. The levels of reactive oxygen species (ROS), malondialdehyde (MDA) and superoxide dismutase (SOD) were determined in the supernatant of A549 cells with ELISA kits (cat. no. E004-1-1; Nanjing Jiancheng Bioengineering Institute), MDA assay kits (cat. no. A003-1-2; Nanjing Jiancheng Bioengineering Institute) and SOD assay kits (cat. no. S0086; Beyotime Institute of Biotechnology) (Beyotime Institute of Biotechnology) according to the manufacturer's instructions.

Statistical analysis. The data are presented as mean ± standard deviation of three independent experimental repeats.

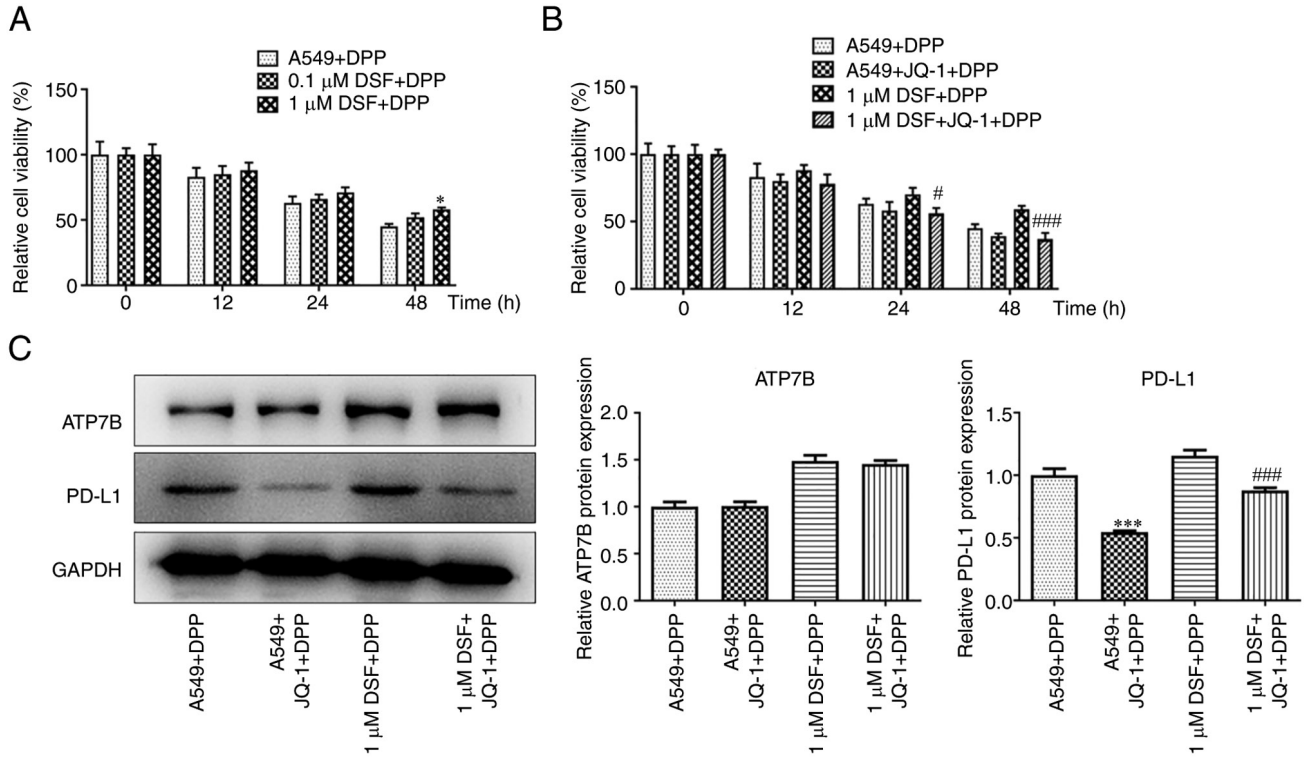

Figure 2. Effect of combination of DSF and JQ-1 on viability and expression of ATP7B and PD-L1 in A549 cells. The viability of DPP-induced A549 cells treated with (A) DSF and (B) JQ-1 and/or DSF was detected by Cell Counting Kit-8 assay. (C) Protein expression of ATP7B and PD-L1 in A549 cells treated with JQ-1 and/or DSF was detected by western blot. *P<0.05, ***P<0.001 vs. A549 + DPP. $^{\#}$P<0.05 and $^{\#\#\#}$P<0.001 vs. 1 μM DSF + DPP. DSF, disulfiram; ATP7B, ATPase copper-transporting β; PD-L1, programmed death-ligand 1; DPP, cisplatin.

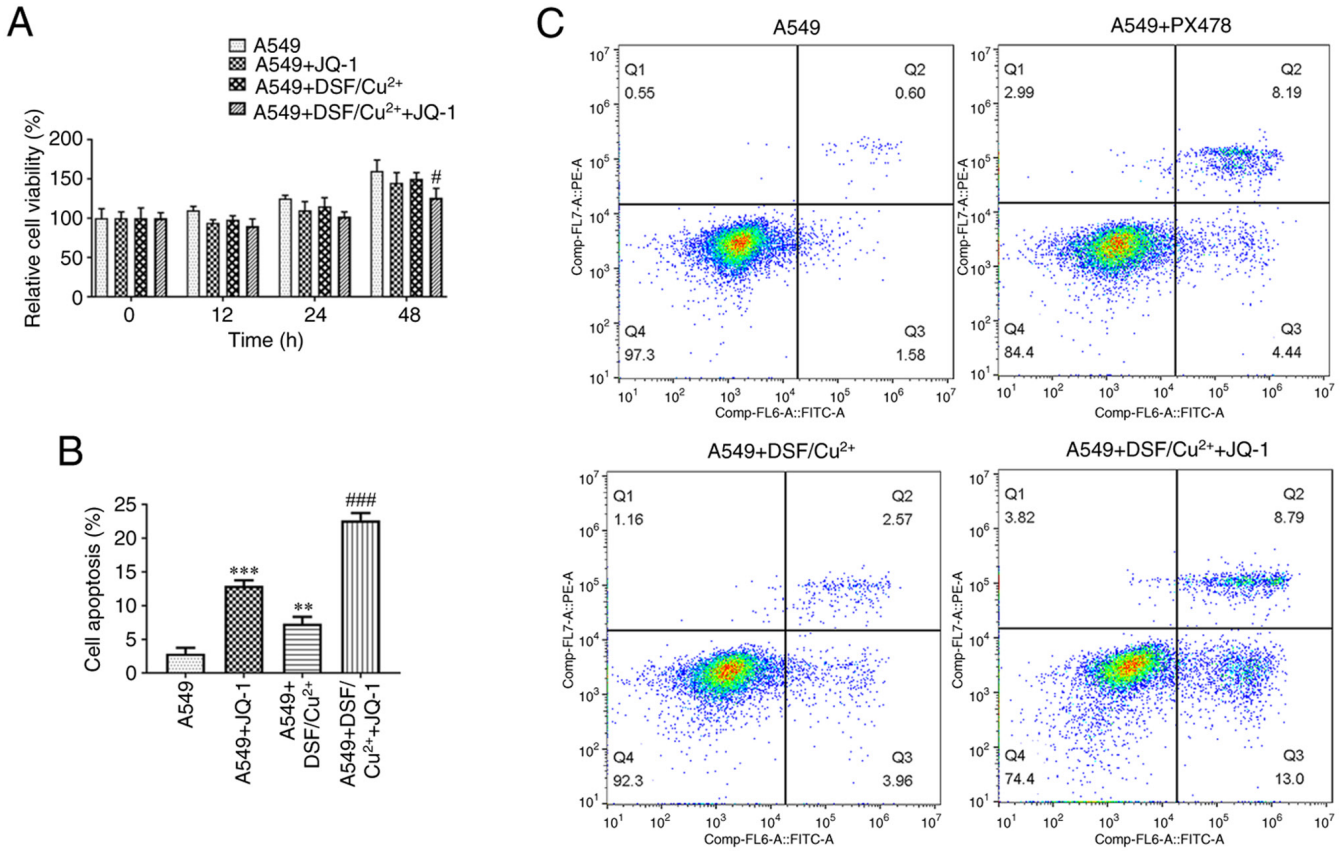

Figure 3. Effect of DSF and/or JQ-1 on viability and apoptosis of A549 cells. (A) Viability of A549 cells treated with DSF/Cu^{2+} and/or JQ-1 was detected by Cell Counting Kit-8 assay. (B) Apoptosis of A549 cells treated with DSF/Cu^{2+} and/or JQ-1 was detected by (C) flow cytometry. **P<0.01, ***P<0.001 vs. A549. $^{\#}$P<0.05, $^{\#\#\#}$P<0.001 vs. A549 + DSF/Cu^{2+}. DSF, disulfiram.

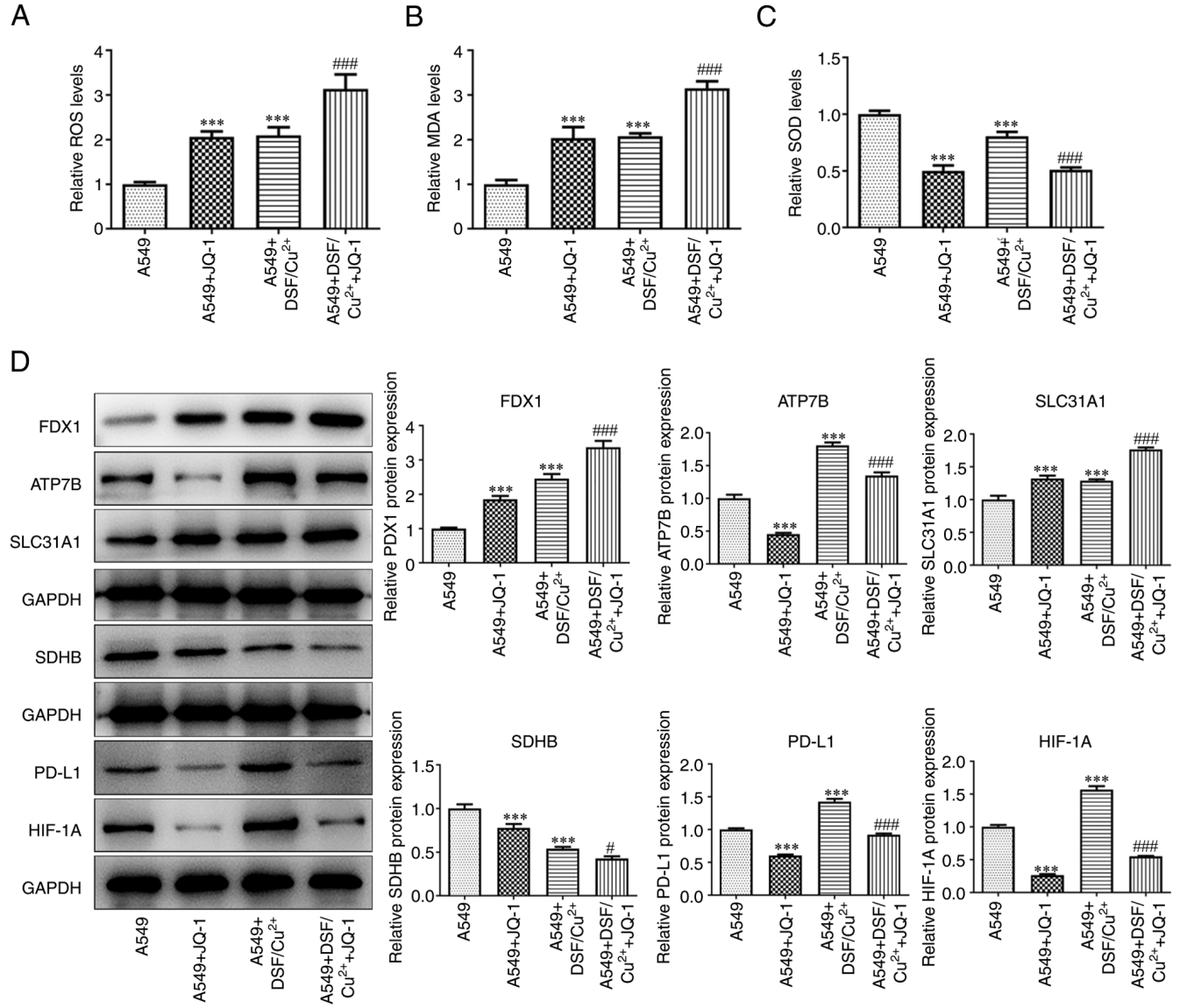

Figure 4. Effect of DSF and/or JQ-1 on oxidative stress and cuproptosis of A549 cells. Levels of (A) ROS, (B) MDA and (C) SOD in A549 cells treated with DSF/Cu^{2+} and/or JQ-1 were detected by commercial assay kits. (D) Expression of cuproptosis-associated proteins in A549 cells treated with DSF/Cu^{2+} and/or JQ-1 was detected by western blot. ***P<0.001 vs. A549. $^{\#}$P<0.05 and $^{\#\#\#}$P<0.001 vs. A549 + DSF/Cu^{2+}. DSF, disulfiram; ROS, reactive oxygen species; MDA, malondialdehyde; SOD, superoxide dismutase; FDX1, ferredoxin-1; ATP7B, ATPase copper-transporting β; SLC31A1, solute carrier family 31 member 1; SDHB, succinate dehydrogenase B; PD-L1, programmed death-ligand 1; HIF-1A, hypoxia inducible factor-1A.

Statistical analysis was performed using GraphPad Prism 8.0.1 (GraphPad Software, Inc.; Dotmatics). Statistical differences were evaluated by one-way analysis of variance followed by Tukey's post hoc test. P<0.05 was considered to indicate a statistically significant difference.

Results

DSF decreases cell viability and upregulated expression levels of ATP7B and PD-L1 of A549 cells. DSF suppressed the viability of A549 cells; the inhibitory effect of DSF on the viability of A549 cells was enhanced by $CuCl_2$ (Fig. 1A). In the presence or absence of $CuCl_2$, the expression levels of ATP7B and PD-L1 were upregulated in A549 cells by DSF (Fig. 1B-D). Not only did $CuCl_2$ significantly inhibit the cell viability, but also significantly up-regulate the expression levels of ATP7B and PD-L1.

The combination treatment of DSF and JQ-1 decreased the viability and the expression of PD-L1 in A549 cells. DSF improved the viability of DPP-treated A549 cells at 48 h (Fig. 2A). JQ-1 suppressed the viability of DPP-treated A549 cells treated with DSF at 24 and 48 h (Fig. 2B). DSF increased expression levels of ATP7B and PD-L1. JQ-1 exhibited no significant effect on ATP7B expression but inhibited expression levels of PD-L1 in DPP-treated A549 cells (Fig. 2C).

The combination treatment of DSF and JQ-1 decreased the viability and induced the apoptosis in A549 cells. Combination of DSF and JQ-1 suppressed the viability of A549 cells (Fig. 3A). JQ-1 promoted the apoptosis of A549 cells and DSF suppressed apoptosis. The combined effect on apoptosis of A549 cells caused by DSF and JQ-1 was more potent than that caused by single treatment of JQ-1 (Fig. 3B and C).

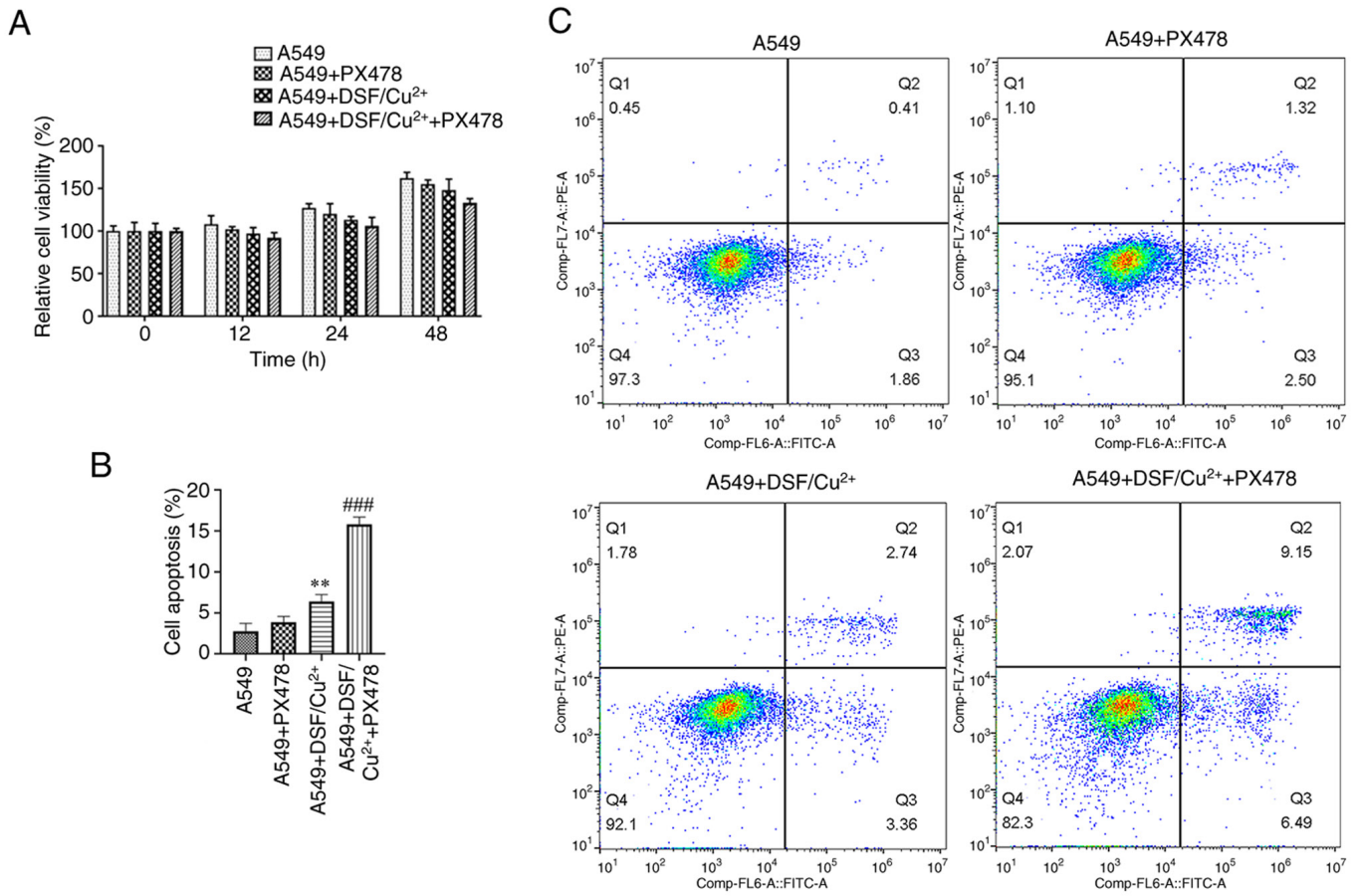

Figure 5. Effect of PX478 on viability and apoptosis of DSF-treated A549 cells. (A) Viability of A549 cells treated with DSF/Cu^{2+} and/or PX478 was detected by Cell Counting Kit-8 assay. (B) Apoptosis of A549 cells treated with DSF/Cu^{2+} and/or PX478 was detected by (C) flow cytometry. **P<0.01 vs. A549. $^{###}$P<0.001 vs. A549 + DSF/Cu^{2+}. DSF, disulfiram.

Combination treatment of DSF and JQ-1 promoted the oxidative stress and cuproptosis of A549 cells. DSF and JQ-1 independently increased levels of ROS and MDA, while decreased levels of SOD in A549 cells. The combined treatment of DSF and JQ-1 further increased levels of ROS and MDA, while decreasing levels of SOD in A549 cells (Fig. 4A-C). JQ-1 upregulated expression of FDX1 and SLC31A1, while it downregulated the expression of ATP7B, SDHB, PD-L1 and HIF-1A in A549 cells. DSF caused an upregulation in expression levels of FDX1, ATP7B, SLC31A1, PD-L1 and HIF-1A, while it downregulated expression levels of SDHB in A549 cells. The combination of DSF and JQ-1 increased expression levels of FDX1 and SLC31A1, while suppressing expression of ATP7B, SDHB, PD-L1 and HIF-1A in A549 cells (Fig. 4D).

PX478 decreases viability and promoted the apoptosis in DSF-treated A549 cells. PX478 increased the effect of DSF and enhanced the inhibitory effect on the viability of A549 cells (Fig. 5A). DSF promoted apoptosis and PX478 enhanced the effect of DSF on the induction of apoptosis in A549 cells (Fig. 5B and C).

PX478 promotes oxidative stress and induced cuproptosis in DSF-treated A549 cells. DSF increased levels of ROS and MDA, while decreasing the levels of SOD in A549 cells. PX478 upregulated the levels of ROS and MDA, while downregulating SOD in DSF-treated A549 cells (Fig. 6A-C). The expression levels of FDX1, ATP7B, SLC31A1, PD-L1, and HIF-1A were increased, while those of SDHB were decreased in A549 cells treated with DSF. PX478 promoted the expression levels of FDX1 and SLC31A1, while suppressing expression levels of ATP7B, PD-L1 and HIF-1A in DSF-treated A549 cells (Fig. 6D).

Discussion

A number of studies have confirmed that DSF exerts anticancer activity via the induction of cell apoptosis by Cu^{2+} (25,26). The present study indicated that DSF/Cu^{2+} inhibited the viability of A549 cells to a greater extent than single treatment with DSF. In the presence or absence of Cu^{2+}, the effects of DSF on the expression levels of ATP7B and PD-L1 were not significant. Hassani *et al* (27) used DSF/Cu to treat acute myeloid leukemia cell lines, confirming that DSF/Cu inhibited the proliferation of these cells in a concentration-dependent manner. Papaioannou *et al* (28) used DSF combined with 1 μmol/l Cu to treat six ovarian cancer cell lines, which promoted cell death.

DSF causes a significant upregulation in expression of PD-L1 in hepatocellular cancer cells, which may enhance immunosuppression and immune escape of tumors (17). The present study indicated that following pretreatment with DSF,

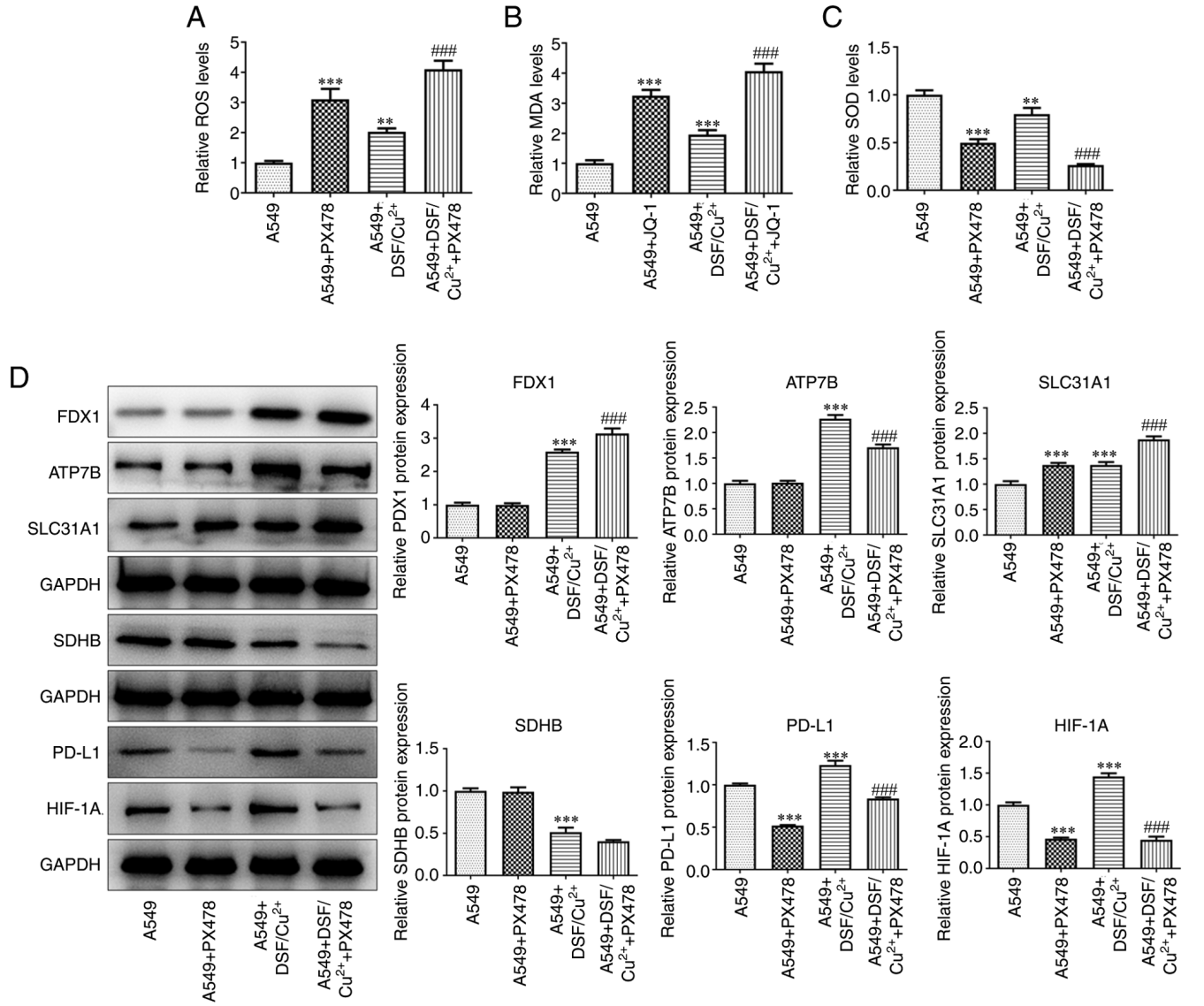

Figure 6. Effect of PX478 on oxidative stress and cuproptosis of DSF-treated A549 cells. Levels of (A) ROS, (B) MDA and (C) SOD in A549 cells treated with DSF/Cu^{2+} and/or PX478 were detected by commercial assay kits. (D) Expression of cuproptosis-associated proteins in A549 cells treated with DSF/Cu^{2+} and/or PX478 was detected by western blot. **P<0.01 and ***P<0.001 vs. A549. $^{###}$P<0.001 vs. A549 + DSF/Cu^{2+}. DSF; ROS, reactive oxygen species; MDA, malondialdehyde; SOD, superoxide dismutase; FDX1, ferredoxin-1; ATP7B, ATPase copper-transporting β; SLC31A1, solute carrier family 31 member 1; SDHB, succinate dehydrogenase B; PD-L1, programmed death-ligand 1; HIF-1A, hypoxia inducible factor-1A.

the viability of DPP-treated A549 cells was improved by upregulating expression levels of ATP7B and PD-L1, which was consistent with previous studies (29,30). It was hypothesized that although DSF independently demonstrated tumor inhibitory activity, it upregulated the expression levels of PD-L1 to enhance immunosuppression and immune escape of tumors.

A previous study indicated that combination of anti-PD-L1 anticancer therapy with DSF promotes the anticancer effect of anti-PD-L1 on breast cancer (29). However, it is possible that the overall anticancer effect may be weakened by upregulation of PD-L1 expression by DSF treatment. Following combined treatment of cells with anti-PD-L1, DSF alone was more efficient in inducing cuproptosis and anticancer effects. Moreover, anti-PD-L1 promoted and improved the anticancer effect of DSF. The present study indicated that addition of JQ-1 (PD-L1 inhibitor) further inhibited viability of A549 cells; however, when A549 cells were pretreated with DSF, JQ-1 reversed the increased DPP resistance of A549 cells caused by upregulation of PD-L1 expression.

A previous study demonstrated that overexpression of ATP7B decreases accumulation and accelerates efflux of Cu, which decreases the effects of DSF on cancer cells. The HIF-1 signaling pathway is suppressed in ATP7B-knockout HepG2 cells (18). HIF-1 is a DNA-binding protein involved in cell signal transduction under hypoxic conditions *in vivo*. The A subunit of HIF-1 is induced and activated by hypoxia to control activity of HIF-1 and regulate its expression (31). PD-L1 is an important factor mediating the immune response of the body. Following combination with PD-1, the expression of tyrosine phosphatase non-receptor type 11 protein is increased via tyrosine-based switch motif to promote phosphorylation of several key molecules of the T cell antigen receptor signaling pathway and inhibit proliferation and activity of T cells. The

expression of PD-L1 on the surface of tumor cells is an important factor leading to immune escape of tumor cells (32,33). Zhao *et al* (34) demonstrated that inhibition of enhancer of zeste homolog 2 expression inhibits the expression of PD-L1 by decreasing levels of HIF-1A, indicating that both PD-L1 and HIF-1A are associated with occurrence and development of NSCLC. Previous studies have shown that HIF-1A induces immune tolerance of tumor cells and promotes malignant development of cancer by regulating PD-L1 expression under hypoxic conditions (35-37). In the present study, HIF-1 inhibitor PX478 was used to investigate the protective effect caused by treatment with DSF on NSCLC. PX478 acted with DSF to suppress cell viability and oxidative stress and promote apoptosis and cuproptosis of A549 cells. However, there are several limitations in the present study. A single cell line, which was established in cell culture, was used; our future experiments will verify the present findings and potential mechanism in other NSCLC cell lines. In addition, the present results require confirmation using animals, as well as clinical studies.

In conclusion, DSF inhibited viability and promoted expression of ATP7B and PD-L1 in A549 cells. The viability of DPP-treated A549 cells was increased following DSF treatment. JQ-1 and PX478 promoted the ability of DSF to suppress cell viability and enhanced the induction of oxidative stress, as well as induction of apoptosis and cuproptosis of A549 cells. Overall, combination of DSF with anti-PD-L1 treatment increased the induction of cuproptosis caused by DSF in NSCLC, which reveals a novel mechanism underlying the combined antitumor effect of DSF with anti-PD-L1 treatment and may facilitate discovery of a lead compound or drug candidate for the development of novel antitumor drugs.

Acknowledgements

Not applicable.

Funding

No funding was received.

Availability of data and materials

The datasets used and/or analyzed during the current study are available from the corresponding author on reasonable request.

Authors' contributions

PL and LZ designed the study and drafted and revised the manuscript. QS, SB and HW analyzed the data and performed the literature review. PL and QS confirmed the authenticity of all the raw data. All authors performed the experiments. All authors have read and approved the final manuscript.

Ethics approval and consent to participate

Not applicable.

Patient consent for publication

Not applicable.

Competing interests

The authors declare that they have no competing interests.

References

1. Siegel RL, Miller KD and Jemal A: Cancer statistics, 2020. CA Cancer J Clin 70: 7-30, 2020.
2. Freeman B, Mamallapalli J, Bian T, Ballas K, Lynch A, Scala A, Huo Z, Fredenburg KM, Bruijnzeel AW, Baglole CJ, *et al*: Opportunities and challenges of kava in lung cancer prevention. Int J Mol Sci 24: 9539, 2023.
3. Akamine T, Toyokawa G, Tagawa T and Seto T: Spotlight on lorlatinib and its potential in the treatment of NSCLC: The evidence to date. Onco Targets Ther 11: 5093-5101, 2018.
4. Chang A: Chemotherapy, chemoresistance and the changing treatment landscape for NSCLC. Lung cancer 71: 3-10, 2011.
5. Miller KD, Siegel RL, Lin CC, Mariotto AB, Kramer JL, Rowland JH, Stein KD, Alteri R and Jemal A: Cancer treatment and survivorship statistics, 2016. CA Cancer J Clin 66: 271-289, 2016.
6. Rossi A and Di Maio M: Platinum-based chemotherapy in advanced non-small-cell lung cancer: Optimal number of treatment cycles. Expert Rev Anticancer Ther 16: 653-660, 2016.
7. Lopez J, Ramchandani D and Vahdat L: Copper depletion as a therapeutic strategy in cancer. Met Ions Life Sci 19: 2019.
8. Bu W, Wang Z, Meng L, Li X, Liu X, Chen Y, Xin Y, Li B and Sun H: Disulfiram inhibits epithelial-mesenchymal transition through TGFβ-ERK-Snail pathway independently of Smad4 to decrease oral squamous cell carcinoma metastasis. Cancer Manag Res 11: 3887-3898, 2019.
9. Li Y, Wang LH, Zhang HT, Wang YT, Liu S, Zhou WL, Yuan XZ, Li TY, Wu CF and Yang JY: Disulfiram combined with copper inhibits metastasis and epithelial-mesenchymal transition in hepatocellular carcinoma through the NF-κB and TGF-β pathways. J Cell Mol Med 22: 439-451, 2018.
10. Bucci M: Cancer therapy: A path of DSF destruction. Nat Chem Biol 14: 107, 2018.
11. Liu X, Wang L, Cui W, Yuan X, Lin L, Cao Q, Wang N, Li Y, Guo W, Zhang X, *et al*: Targeting ALDH1A1 by disulfiram/copper complex inhibits non-small cell lung cancer recurrence driven by ALDH-positive cancer stem cells. Oncotarget 7: 58516-58530, 2016.
12. Morrison BW, Doudican NA, Patel KR and Orlow SJ: Disulfiram induces copper-dependent stimulation of reactive oxygen species and activation of the extrinsic apoptotic pathway in melanoma. Melanoma Res 20: 11-20, 2010.
13. Liu P, Brown S, Goktug T, Channathodiyil P, Kannappan V, Hugnot JP, Guichet PO, Bian X, Armesilla AL, Darling JL and Wang W: Cytotoxic effect of disulfiram/copper on human glioblastoma cell lines and ALDH-positive cancer-stem-like cells. Br J Cancer 107: 1488-1497, 2012.
14. Cheriyan VT, Wang Y, Muthu M, Jamal S, Chen D, Yang H, Polin LA, Tarca AL, Pass HI, Dou QP, *et al*: Disulfiram suppresses growth of the malignant pleural mesothelioma cells in part by inducing apoptosis. PLoS One 9: e93711, 2014.
15. Skrott Z, Mistrik M, Andersen KK, Friis S, Majera D, Gursky J, Ozdian T, Bartkova J, Turi Z, Moudry P, *et al*: Alcohol-abuse drug disulfiram targets cancer via p97 segregase adaptor NPL4. Nature 552: 194-199, 2017.
16. Tsvetkov P, Coy S, Petrova B, Dreishpoon M, Verma A, Abdusamad M, Rossen J, Joesch-Cohen L, Humeidi R, Spangler RD, *et al*: Copper induces cell death by targeting lipoylated TCA cycle proteins. Science 375: 1254-1261, 2022.
17. Zhou B, Guo L, Zhang B, Liu S, Zhang K, Yan J, Zhang W, Yu M, Chen Z, Xu Y, *et al*: Disulfiram combined with copper induces immunosuppression via PD-L1 stabilization in hepatocellular carcinoma. Am J Cancer Res 9: 2442-2455, 2019.
18. Mi X, Li Z, Yan J, Li Y, Zheng J, Zhuang Z, Yang W, Gong L and Shi J: Activation of HIF-1 signaling ameliorates liver steatosis in zebrafish atp7b deficiency (Wilson's disease) models. Biochim Biophys Acta Mol Basis Dis 1866: 165842, 2020.
19. Luo F, Lu FT, Cao JX, Ma WJ, Xia ZF, Zhan JH, Zeng KM, Huang Y, Zhao HY and Zhang L: HIF-1α inhibition promotes the efficacy of immune checkpoint blockade in the treatment of non-small cell lung cancer. Cancer Lett 531: 39-56, 2022.

20. Sun S, Guo C, Gao T, Ma D, Su X, Pang Q and Zhang R: Hypoxia enhances glioma resistance to sulfasalazine-induced ferroptosis by upregulating SLC7A11 via PI3K/AKT/HIF-1α Axis. Oxid Med Cell Longev 2022: 7862430, 2022.
21. Koh MY, Spivak-Kroizman T, Venturini S, Welsh S, Williams RR, Kirkpatrick DL and Powis G: Molecular mechanisms for the activity of PX-478, an antitumor inhibitor of the hypoxia-inducible factor-1alpha. Mol Cancer Ther 7: 90-100, 2008.
22. Cui Z, Ruan Z, Li M, Ren R, Ma Y, Zeng J, Sun J, Ye W, Xu W, Guo X, *et al*: Intermittent hypoxia inhibits anti-tumor immune response via regulating PD-L1 expression in lung cancer cells and tumor-associated macrophages. Int Immunopharmacol 122: 110652, 2023.
23. Walter B, Gil S, Naizhen X, Kruhlak MJ, Linehan WM, Srinivasan R and Merino MJ: Determination of the expression of PD-L1 in the morphologic spectrum of renal cell carcinoma. J Cancer 11: 3596-3603, 2020.
24. Livak KJ and Schmittgen TD: Analysis of relative gene expression data using real-time quantitative PCR and the 2(-Delta Delta C(T)) Method. Methods 25: 402-408, 2001.
25. Xu R, Zhang K, Liang J, Gao F, Li J and Guan F: Hyaluronic acid/polyethyleneimine nanoparticles loaded with copper ion and disulfiram for esophageal cancer. Carbohydr Polym 261: 117846, 2021.
26. Chen SY, Chang YL, Liu ST, Chen GS, Lee SP and Huang SM: Differential cytotoxicity mechanisms of copper complexed with disulfiram in oral cancer cells. Int J Mol Sci 22: 3711, 2021.
27. Hassani S, Ghaffari P, Chahardouli B, Alimoghaddam K, Ghavamzadeh A, Alizadeh S and Ghaffari SH: Disulfiram/copper causes ROS levels alteration, cell cycle inhibition, and apoptosis in acute myeloid leukaemia cell lines with modulation in the expression of related genes. Biomed Pharmacother 99: 561-569, 2018.
28. Papaioannou M, Mylonas I, Kast RE and Brüning A: Disulfiram/copper causes redox-related proteotoxicity and concomitant heat shock response in ovarian cancer cells that is augmented by auranofin-mediated thioredoxin inhibition. Oncoscience 1: 21-29, 2013.
29. Zheng X, Liu Z, Mi M, Wen Q, Wu G and Zhang L: Disulfiram Improves the Anti-PD-1 Therapy Efficacy by Regulating PD-L1 expression via epigenetically reactivation of IRF7 in triple negative breast cancer. Front Oncol 11: 734853, 2021.
30. Falls-Hubert KC, Butler AL, Gui K, Anderson M, Li M, Stolwijk JM, Rodman SN III, Solst SR, Tomanek-Chalkley A, Searby CC, *et al*: Disulfiram causes selective hypoxic cancer cell toxicity and radio-chemo-sensitization via redox cycling of copper. Free Radic Biol Med 150: 1-11, 2020.
31. Du H, Chen Y, Hou X, Huang Y, Wei X, Yu X, Feng S, Wu Y, Zhan M, Shi X, *et al*: PLOD2 regulated by transcription factor FOXA1 promotes metastasis in NSCLC. Cell Death Dis 8: e3143, 2017.
32. Patsoukis N, Brown J, Petkova V, Liu F, Li L and Boussiotis VA: Selective effects of PD-1 on Akt and Ras pathways regulate molecular components of the cell cycle and inhibit T cell proliferation. Sci Signal 5: ra46, 2012.
33. Munari E, Zamboni G, Marconi M, Sommaggio M, Brunelli M, Martignoni G, Netto GJ, Moretta F, Mingari MC, Salgarello M, *et al*: PD-L1 expression heterogeneity in non-small cell lung cancer: Evaluation of small biopsies reliability. Oncotarget 8: 90123-90131, 2017.
34. Zhao Y, Wang XX, Wu W, Long H, Huang J, Wang Z, Li T, Tang S, Zhu B and Chen D: EZH2 regulates PD-L1 expression via HIF-1α in non-small cell lung cancer cells. Biochem Biophys Res Commun 517: 201-209, 2019.
35. Noman MZ, Desantis G, Janji B, Hasmim M, Karray S, Dessen P, Bronte V and Chouaib S: PD-L1 is a novel direct target of HIF-1α, and its blockade under hypoxia enhanced MDSC-mediated T cell activation. J Exp Med 211: 781-790, 2014.
36. Daniel SK, Sullivan KM, Labadie KP and Pillarisetty VG: Hypoxia as a barrier to immunotherapy in pancreatic adenocarcinoma. Clin Transl Med 8: 10, 2019.
37. Barsoum IB, Smallwood CA, Siemens DR and Graham CH: A mechanism of hypoxia-mediated escape from adaptive immunity in cancer cells. Cancer Res 74: 665-674, 2014.